[^{13}C]-Enriched Methyl Aldopyranosides: Structural Interpretations of ^{13}C−^{1}H Spin-Coupling Constants and ^{1}H Chemical Shifts

Carol A. Podlasek,‡ Jian Wu,† Wayne A. Stripe,‡ Paul B. Bondo,§ and Anthony S. Serianni*,‡

Contribution from the Department of Chemistry and Biochemistry, University of Notre Dame, Notre Dame, Indiana 46556, Department of Chemistry, Purdue University, West Lafayette, Indiana 47907, and Omicron Biochemicals, Inc., South Bend, Indiana 46637

Received January 30, 1995®

Abstract: A series of methyl D-aldopentopyranosides and D-aldohexopyranosides having different configurations has been synthesized with single sites of ^{13}C-enrichment at various sites, and one-, two-, and three-bond ^{13}C−^{1}H spin-coupling constants ($^{1}J_{CH}$, $^{2}J_{CH}$, and $^{3}J_{CH}$) in these compounds have been obtained in $^{2}H_2O$ by 1-D and/or 2-D NMR methods. The effects of ring configuration and conformation on these J_{CH} values were assessed with the aim of identifying specific structural features that affect their magnitudes and signs. ^{1}H chemical shifts for the same compounds were also measured, and the data were used to derive empirical relationships between chemical shift and aldopyranosyl ring configuration. The correlations obtained on these conformationally-stable glycosides have implications for the interpretation of similar NMR parameters in biologically-important oligosaccharides and in conformationally flexible aldofuranosyl rings such as those found in DNA and RNA.

Introduction

Vicinal ^{1}H−^{1}H spin-spin coupling constants ($^{3}J_{HH}$) and ^{1}H chemical shifts have played key roles in the assignment of configuration and conformation of aldopyranosyl rings, the latter existing either as free entities (e.g., monosaccharides) or as constituents of complex biologically-important structures (e.g., oligosaccharides).[1,2] These parameters can be extracted from 1-D and multidimensional (MD) ^{1}H NMR spectra,[3,4] and, in the case of $^{3}J_{HH}$, related to molecular structure and conformation via appropriate Karplus relationships.[5,6] ^{1}H chemical shift has been confined, for the most part, to the use of structural "reporter groups", as first described by Vliegenthart and co-workers,[7] which assist in the identification of specific residues in oligosaccharides. Despite their undisputed value in the latter regard, the effect of structure and configuration on the ^{1}H chemical shifts of aldopyranosyl rings is not fully understood.

The rapid advances made in protein structure determination over the past decade may be attributed, in large part, to the combined use of stable isotopes and MD NMR methods,[8,9] and a similar strategy is currently being applied to nucleic acids.[10] The same combined methodology is likely to be valuable in structural studies of complex carbohydrates. The presence of ^{13}C-enrichment, either site-specific or uniform, facilitates the use of heteronuclear MD NMR methods capable of deciphering complex spectra such as those exhibited by oligosaccharides. In practice, the problem of signal assignment and analysis is often more acute in ^{1}H NMR spectra of oligosaccharides than in those of proteins and nucleic acids, since the former show not only poor signal dispersion but also non-first-order behavior even at high fields (≥600 MHz).

In addition to facilitating spectral interpretation, ^{13}C-labeling is helpful in evaluating key conformational elements of oligosaccharides. For example, ^{13}C−^{13}C and ^{13}C−^{1}H spin-couplings are the only J values available to assess O-glycoside linkage conformation,[11] and these couplings, especially the former, are most easily measured in appropriately ^{13}C-labeled molecules. Furthermore, these spin-couplings, when used in conjunction with more conventional NMR parameters, provide an improved means to study molecules that are conformationally flexible.[11c,12]

One- ($^{1}J_{CH}$), two- ($^{2}J_{CH}$), and three- ($^{3}J_{CH}$) bond ^{13}C−^{1}H spin-couplings have been measured previously in monosaccharides and oligosaccharides,[11−14] although their relationship to aldopyranosyl ring structure and configuration has not been fully explored. Apart from the current difficulties in the measurement of J_{CH} in unlabeled compounds,[15] this lack of detailed knowledge confines these couplings to qualitative, or at best semi-quantitative, treatments in structural studies of carbohydrate-containing molecules. In this investigation, ^{13}C−^{1}H spin-coupling behavior involving various carbons of 30 ^{13}C-labeled

* Author to whom correspondence should be addressed.
† Purdue University.
‡ University of Notre Dame.
§ Omicron Biochemicals, Inc.
® Abstract published in *Advance ACS Abstracts,* August 1, 1995.

(1) Booth, H. *Prog. NMR Spectrosc.* **1969**, *5*, 149.
(2) Bentley, R. *Ann. Rev. Biochem.* **1972**, *41*, 953.
(3) Zhou, N.; Manogaran, S.; Zon, G.; James, T. L. *Biochemistry* **1988**, *27*, 6013.
(4) Griesinger, C.; Eggenberger, U. *J. Magn. Reson.* **1992**, *97*, 426.
(5) Karplus, M. *J. Chem. Phys.* **1959**, *30*, 11.
(6) (a) Haasnoot, C. A. G.; de Leeuw, F. A. A. M.; Altona, C. *Tetrahedron* **1980**, *36*, 2783. (b) Haasnoot, C. A. G.; de Leeuw, F. A. A. M.; de Leeuw, H. P. M.; Altona, C. *Org. Magn. Reson.* **1981**, *15*, 43.
(7) Vliegenthart, J. F. G.; Dorland, L.; van Halbeek, H. *Adv. Carbohydr. Chem. Biochem.* **1983**, *41*, 209.
(8) (a) Otting, G.; Wuthrich, K. *Quart. Rev. Biophys.* **1990**, *23*, 39. (b) Fesik, S. W.; Zuiderweg, E. R. P. *Quart. Rev. Biophys.* **1990**, *23*, 97.
(9) Clore, G. M.; Gronenborn, A. M. *Prog. NMR Spectrosc.* **1991**, *23*, 43.
(10) (a) Hines, J. V.; Varani, G.; Landry, S. M.; Tinoco, Jr., I. *J. Am. Chem. Soc.* **1993**, *115*, 11002. (b) Lancelot, G.; Chanteloup, L.; Beau, J. M.; Thuong, N. T. *J. Am. Chem. Soc.* **1993**, *115*, 1599. (c) Legault, P.; Farmer II, B. T.; Mueller, L.; Pardi, A. *J. Am. Chem. Soc.* **1994**, *116*, 2203. (d) Marino, J. P.; Prestegard, J. H.; Crothers, D. M. *J. Am. Chem. Soc.* **1994**, *116*, 2205.
(11) (a) Nunez, H. A.; Barker, R. *Biochemistry* **1980**, *19*, 489. (b) Rosevear, P. R.; Nunez, H. A.; Barker, R. *Biochemistry* **1982**, *21*, 1421. (c) Hayes, M. L.; Serianni, A. S.; Barker, R. *Carbohydr. Res.* **1982**, *100*, 87.
(12) Duker, J.; Serianni, A. S. *Carbohydr. Res.* **1993**, *249*, 281.

0002-7863/95/1517-8635$09.00/0

Table 1. ^1H-^1H Spin-Coupling Constants[a] in Methyl Aldopyranosides

	coupled nuclei						
compound	H1-H2	H2-H3	H3-H4	H4-H5	H5-H6 (H4-H5′)	H5-H6 (H5-H5′)	H6-H6′
α-*allo*	4.0	~3.7	3.1	10.1	~1.9	obs[b]	~−11.9
β-*allo*	8.3	3.1	3.0	10.1	2.2	6.1	−12.2
β-*altro*	1.6	4.8	~2.8	~12.0	obs	5.7	~−11.9
β-*arabino*	3.8	10.1	3.5	1.5	2.1	−12.8	
α-*galacto*	4.0	10.3	3.4	1.0	7.2	5.2	−11.7
β-*galacto*	7.9	9.9	3.4	1.1	7.9	4.4	−11.7
α-*gluco*	3.8	9.8	9.1	10.1	2.3	5.5	−12.3
β-*gluco*	8.0	9.4	9.2	9.7	2.3	6.0	−12.3
α-*manno*	1.8	3.5	9.5	obs	2.1	5.9	−12.2
β-*manno*	0.9	3.2	9.6	9.7	2.4	6.5	−12.2
α-*talo*	~1.9	3.4	~3.5	~1.3	7.7	3.9	−11.2
α-*xylo*	3.6						
β-*xylo*	7.8	9.3	9.1	5.5	10.5	−11.6	

[a] In ^2H_2O, 30 °C; accurate to ±0.1 Hz. Values preceded by a ~ symbol are accurate to ±0.3 Hz. [b] Entry "obs" denotes obscured signals from which the particular $^3J_{HH}$ could not be measured.

methyl aldopento- and aldohexopyranosides has been examined in order to refine the relationships between coupling magnitude and aldopyranosyl ring structure. In the course of this work, ^1H chemical shifts were also recorded under identical solution conditions, permitting an assessment of empirical correlations to aldopyranosyl ring structure.

Experimental Section

Compounds. Methyl α-D-[1-^{13}C]allopyranoside, methyl β-D-[1-^{13}C]-allopyranoside, methyl β-D-[1-^{13}C]altropyranoside, methyl α-D-[1-^{13}C]arabinopyranoside, methyl β-D-[1-^{13}C]arabinopyranoside, methyl β-D-[1-^{13}C]galactopyranoside, methyl α-D-[1-^{13}C]glucopyranoside, methyl β-D-[1-^{13}C]glucopyranoside, methyl α-D-[1-^{13}C]mannopyranoside, methyl β-D-[1-^{13}C]mannopyranoside, methyl α-D-[1-^{13}C]xylopyranoside, methyl β-D-[1-^{13}C]xylopyranoside, methyl α-D-[2-^{13}C]allopyranoside, methyl β-D-[2-^{13}C]allopyranoside, methyl β-D-[2-^{13}C]arabinopyranoside, methyl α-D-[2-^{13}C]galactopyranoside, methyl β-D-[2-^{13}C]-galactopyranoside, methyl α-D-[2-^{13}C]glucopyranoside, methyl β-D-[2-^{13}C]glucopyranoside, methyl α-D-[2-^{13}C]mannopyranoside, methyl β-D-[2-^{13}C]mannopyranoside, methyl α-D-[2-^{13}C]talopyranoside, methyl β-D-[3-^{13}C]allopyranoside, methyl α-D-[3-^{13}C]glucopyranoside, methyl β-D-[3-^{13}C]glucopyranoside, methyl α-D-[3-^{13}C]mannopyranoside, methyl β-D-[3-^{13}C]mannopyranoside, methyl α-D-[4-^{13}C]glucopyranoside, methyl β-D-[5-^{13}C]glucopyranoside, methyl β-D-[6-^{13}C]glucopyranoside, and D-[5-^{13}C]glucose were prepared and purified according to methods described previously,[16a-c] and only an outline of procedures is described here. [^{13}C]Labeled aldoses were prepared by cyanohydrin reduction[16a,b] and/or molybdate epimerization,[16b,17] and purification was achieved by chromatography on Dowex 50 × 8 (200−400 mesh) ion-exchange resin in the Ca^{2+} form;[18a] compounds labeled at C-4 and C-5 were prepared by chemi-enzymic methods from [^{13}C]labeled DL-glyceraldehyde.[16b] The purified labeled aldoses (~0.7 g) were dissolved in 50 mL of anhydrous methanol, 1 g of dry Dowex 50 × 8 (200−400 mesh) ion-exchange resin in the H^+ form was added, and the suspension was refluxed for 1−2 days. After filtration to remove the resin, the methanolic solution containing a mixture of pyranosides and furanosides was concentrated to dryness, and the residue was dissolved in a minimum quantity of distilled water and applied to a column of Dowex 1 × 8 (200−400 mesh) ion-exchange resin in the OH^- form.[18b] The column was eluted with distilled, decarbonated water, and fractions were assayed with phenol-sulfuric acid.[18c] Fractions containing sugar were pooled and evaporated to dryness at 30 °C *in vacuo*. Identification of anomers was made by comparison of ^{13}C chemical shifts obtained for the ^{13}C-labeled compounds with those reported previously[19] and by analysis of $^3J_{HH}$ data (Table 1).

NMR Spectroscopy. High-resolution ^1H NMR spectra were obtained on a Varian VXR-500S (UNITY) FT-NMR spectrometer or a Varian VXR-600 (UNITY) FT-NMR spectometer operating at 30 °C. Samples (15 mM) were exchanged three times with ^2H_2O (99.8 atom % ^2H, Cambridge Isotope Laboratories) and dissolved in 0.6 mL of ^2H_2O, and the solutions were transferred to 5 mm NMR tubes (Wilmad) and sealed with plastic caps.

Measurement of ^1H Chemical Shifts, and ^1H-^1H and ^{13}C−^1H Spin-Coupling Constants. In most cases, ^1H chemical shifts and ^1H-^1H and ^{13}C−^1H spin-coupling constants were measured directly from 1-D ^1H NMR spectra via signal multiplet analysis. In cases where measurement was complicated by signal overlap and/or non-first-order behavior, use was made of homonuclear 2-D *J* spectra,[20,21] ^1H-^1H COSY or TOCSY,[22-24] ^1H-coupled ^{13}C NMR spectra[25] and/or spectral simulation (LAOCN5 as implemented in the FT-NMR program, VAX version, Hare Research, Woodinville, WA) to extract accurate couplings.

The signs of $^2J_{CH}$ values were either measured directly via the 2D homonuclear crosspeak displacement method[26,27] or were predicted using the projection rule of Bock and Pedersen.[13c] According to the

(13) (a) Bock, K.; Lundt, I.; Pedersen, C. *Tetrahedron Lett.* **1973**, 1037. (b) Bock, K.; Pedersen, C. *Acta Chem. Scand. Ser. B* **1975**, *B29*, 258. (c) Bock, K.; Pedersen, C. *Acta Chem. Scand. Ser. B* **1977**, *B31*, 354. (d) Canes, F. H.; Foces-Foces, C.; Jimenez-Barbero, J.; Alemany, A.; Bernabe, M.; Martin-Lomas, M. *J. Org. Chem.* **1987**, *52*, 3367. (e) Hamer, G. K.; Balza, F.; Cyr, N.; Perlin, A. S. *Can. J. Chem.* **1978**, *56*, 3109. (f) Schwarcz, J. A.; Perlin, A. S. *Can. J. Chem.* **1972**, *50*, 3667. (g) Schwarcz, J. A.; Cyr, N.; Perlin, A. S. *Can. J. Chem.* **1975**, *53*, 1872. (h) Barker, R.; Walker, T. E. *Methods Carbohydr. Chem.* **1980**, *8*, 151. (i) Mulloy, B.; Frenkiel, T. A.; Davies, D. B. *Carbohydr. Res.* **1988**, *184*, 39. (j) Tvaroska, I.; Hricovini, H.; Petrakova, E. *Carbohydr. Res.* **1989**, *189*, 359. (k) Walker, T. E.; London, R. E.; Whaley, T. W.; Barker, R.; Matwiyoff, N.A. *J. Am. Chem. Soc.* **1976**, *98*, 5807. (l) Spoormaker, T.; de Bie, M. J. A. *Rec. Trav. Chim. Pays-Bas.* **1978**, 97, 85.

(14) Ichikawa, Y.; Lin Y.-C.; Dumas, D. P.; Shen, G.-H.; Garcia-Junceda, E.; Williams, M. A.; Bayer, R.; Ketcham, C.; Walker, L. E.; Paulson, J. C.; Wong, C.-H. *J. Am. Chem. Soc.* **1992**, *114*, 9283.

(15) (a) Zhu, G.; Renwick, A.; Bax, A. *J. Magn. Reson. Series A* **1994**, 110, 257. (b) Nuzillard, J.-M.; Freeman, R. *J. Magn. Reson. Series A* **1994**, 110, 262. (c) Morat, C.; Taravel, F. R.; Vignon, M. R. *Magn. Reson. Chem.* **1988**, 26, 264.

(16) (a) Serianni, A. S.; Nunez, H. A.; Barker, R. *Carbohydr. Res.* **1979**, *72*, 71. (b) Serianni, A. S.; Vuorinen, T.; Bondo, P. B. *J. Carbohydr. Chem.* **1990**, *9*, 513. (c) King-Morris, M. J.; Bondo, P. B.; Mrowca, R. A.; Serianni, A. S. *Carbohydr. Res.* **1988**, *175*, 49.

(17) Hayes, M. L.; Pennings, N. J.; Serianni, A. S.; Barker, R. *J. Am. Chem. Soc.* **1982**, *104*, 6764.

(18) (a) Angyal, S. J.; Bethell, G. S.; Beveridge, R. *Carbohydr. Res.* **1979**, *73*, 9. (b) Austin, P. W.; Hardy, F. E.; Buchanan, J. C.; Baddiley, J. *J. Chem. Soc.* **1963**, 5350. (c) Hodge, J. E.; Hofreiter, B. T. *Methods Carbohydr. Chem.* **1962**, *1*, 380.

(19) Bock, K.; Pedersen, C. *Adv. Carbohydr. Chem. Biochem.* **1983**, *41*, 27.

(20) (a) Aue, W. P.; Karhan, J.; Ernst, R. R. *J. Chem. Phys.* **1976**, *64*, 4226. (b) Bax, A.; Mehlkopf, A. F.; Smidt, J. *J. Magn. Reson.* **1980**, *40*, 213.

(21) Vuorinen, T.; Serianni, A. S. *Carbohydr. Res.* **1990**, *207*, 185.

(22) Jeener, J. Ampere International Summer School II, Basko Polje, Yugoslavia, 1971.

(23) Bax, A.; Freeman, R. *J. Magn. Reson.* **1981**, *42*, 164.

(24) Braunschweiler, L.; Ernst, R. R. *J. Magn. Reson.* **1983**, *53*, 521.

(25) Garrett, E. C.; Serianni, A. S. *Carbohydr. Res.* **1990**, *208*, 23.

Chart 1

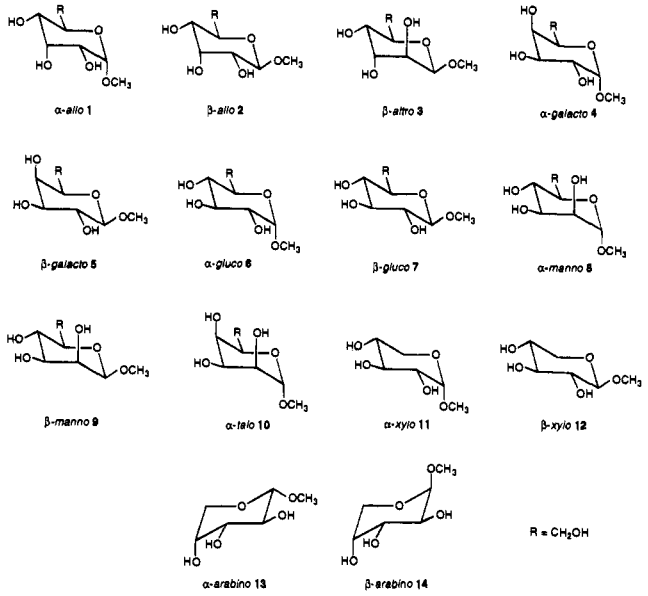

latter rule, a Newman projection viewed from ^{13}C to ^{12}C is made, and the C−O bonds are projected on an axis *trans* to the ^{12}C−^{1}H bond. The sum of the cosines of the angle each oxygen makes with this axis (the projection sum) is used to predict the magnitude and sign of $^{2}J_{CH}$. For example, the relevant projection for $^{2}J_{C1,H2}$ in methyl β-D-[1-^{13}C]-allopyranoside (Figure 1) gives a projection sum of cos 120° + cos 120° + cos 60° = −0.5, yielding a predicted $^{2}J_{C1,H2}$ of ∼−5 Hz.

^{1}H-^{1}H and ^{13}C−^{1}H spin-coupling constants reported as 0 Hz in Tables 1−4 refer to couplings <0.5 Hz, the latter being the estimated lower limit of resolution in these studies, unless otherwise indicated.

Conformations of Methyl Aldopyranosides. Fourteen methyl D-aldopyranosides were examined in this study, four being pentopyranosides and the remainder hexopyranosides. These compounds were chosen in part because they are conformationally stable, that is, they highly favor one chair form in aqueous solution,[28ab] thus eliminating the potential problem of conformational heterogeneity when interpreting NMR parameters. Their structures are shown in Chart 1. Those compounds favoring $^{4}C_1$ conformations include methyl α-D-allopyranoside **1**, methyl β-D-allopyranoside **2**, methyl β-D-altropyranoside **3**, methyl α-D-galactopyranoside **4**, methyl β-D-galactopyranoside **5**, methyl α-D-glucopyranoside **6**, methyl β-D-glucopyranoside **7**, methyl α-D-mannopyranoside **8**, methyl β-D-mannopyranoside **9**, methyl α-D-talopyranoside **10**, methyl α-D-xylopyranoside **11**, and methyl β-D-xylopyranoside **12**. Compounds favoring the $^{1}C_4$ conformation include methyl α-D-arabinopyranoside **13** and methyl β-D-arabinopyranoside **14**. These compounds were singly labeled with ^{13}C at various carbons, producing 30 labeled glycosides with which to evaluate J_{CH} values at a range of carbons within the aldopyranosyl ring. Throughout this paper, the above-noted compounds are denoted as α-*allo* (methyl α-D-allopyranoside), β-*allo* (methyl β-D-allopyranoside), and so forth.

Neutron diffraction studies of methyl α-D-galactopyranoside monohydrate,[28c] methyl β-D-galactopyranoside,[28c] methyl α-D-glucopyranoside,[28d] methyl α-D-mannopyranoside,[28d] and methyl β-D-xylopyranoside[28e] have been reported, and X-ray crystallographic structures are available for methyl α-L-arabinopyranoside,[28f] methyl β-L-arabinopyranoside,[28f] methyl β-D-glucopyranoside hemihydrate,[28g] and methyl α-D-xylopyranoside.[28h] These structural data have been used in the analysis of $^{3}J_{CH}$ values with the understanding that correlations drawn between these values and structural parameters observed in the crystalline state are subject to some error, since crystal packing forces may, in some instances, lead to deformations not found in the solution state.

Results and Discussion

(A) ^{13}C−^{1}H Spin-Coupling Constants. (a) Couplings Involving C-1. $^{1}J_{C1,H1}$ varies with anomeric configuration, with equatorial C-1−H-1 bonds giving couplings (170.1 ± 0.6 Hz)[29] about 10 Hz larger than axial C-1−H-1 bonds (161.5 ± 1.2 Hz) as observed previously[13a,b] (Table 2). $^{1}J_{C1,H1}$ observed in α-*arabino* (161.1 Hz) and β-*arabino* (169.7 Hz) provide evidence that these compounds prefer the $^{1}C_4$ ring conformation; additional longer range ^{13}C−^{1}H couplings confirm this ring geometry as discussed below.

Small absolute $^{2}J_{C1,H2}$ values are observed for α-*allo*, β-*altro*, α-*gluco*, α-*manno*, and β-*manno* (1.0 ± 0.6 Hz), whereas larger absolute values are observed for β-*allo*, α-*arabino*, β-*galacto*, β-*gluco*, and β-*xylo* (6.2 ± 0.3 Hz) (Table 2). Previous studies have shown that the sign of $^{2}J_{C1,H2}$ in β-*allo* is negative[13g,27] as predicted by the projection rule proposed by Bock and Pedersen.[13c] Since the C-1−C-2 rotamers for β-*allo*, α-*arabino*, β-*galacto*, β-*gluco*, and β-*xylo* are identical and since the substitution pattern on the C−C−H fragment is a critical determinant of $^{2}J_{CH}$,[13c,f,g] $^{2}J_{C1,H2}$ in all of these compounds is probably negative. The C-1−C-2 rotamers for α-*allo*, β-*altro*, α-*gluco*, α-*manno*, and β-*manno* are also structurally related, and the projection rule[13c] predicts positive signs for $^{2}J_{C1,H2}$ in these configurations. However, the sign for the α-*manno* configuration was found to be *negative* by the crosspeak displacement method,[26,27] and thus other $^{2}J_{C1,H2}$ values in this group may also be negative. As observed throughout this investigation, the projection rule[13c] gives reliable predictions of $^{2}J_{CH}$ *sign* only when the observed coupling is comparatively large (absolute value >2−3 Hz); sign predictions for smaller couplings must be verified by experiment.

Coupling between C-1 and H-3 is expected to depend on the C-2−C-3 torsion angle.[13f,l] Indeed, large couplings are observed in α-*allo*, β-*allo*, and β-*altro* (5.5 ± 0.5 Hz) in which C-1 and H-3 are antiperiplanar or nearly so (Table 2). In structures having the β-*galacto*, α-*gluco*, β-*gluco*, α-*manno*, β-*manno*, and β-*xylo* configurations, $^{3}J_{C1,H3}$ is small (0.7 ± 0.7 Hz) and reflects a dihedral angle between C-1 and H-3 of ∼60° in these compounds (i.e., C-1 and H-3 are gauche) (Table 2). The variability of $^{3}J_{C1,H3}$ within these two groups probably arises from slight differences in ring torsion angles and/or small substituent effects on ^{13}C−^{1}H couplings. Torsion angles between C-1 and H-3 ($\Theta_{C1,H3}$) derived from crystallographic studies are as follows: β-*galacto* (66.2°),[28c] α-*gluco* (64.0°),[28d] β-*gluco* (65.5°),[28g] α-*manno* (65.8°),[28d] and β-*xylo* (67.1°).[28e] The variation in $\Theta_{C1,H3}$ within this group is small (3.1°) and does not appear to explain the observed variations in $^{3}J_{C1,H3\ (gauche)}$ (i.e., smaller $\Theta_{C1,H3}$ should translate into larger $^{3}J_{C1,H3\ (gauche)}$, but this correlation is not consistently observed in the data). $^{3}J_{C1,H3\ (gauche)}$ appears to be affected by configuration at the intervening C-2, *with an equatorial OH group increasing the observed coupling* (e.g., conversion of β-*manno* to β-*gluco*). A similar effect may also be present for $^{3}J_{C1,H3\ (antiperiplanar)}$ (e.g., coupling increases in the conversion of β-*altro* to β-*allo*). The orientation of O-1 with respect to the coupling pathway may also influence $^{3}J_{C1,H3}$, with coupling pathways having O-1 in the C-1−C-2−C-3 plane (β-D-configurations) increasing the

(26) Montelione, G. T.; Winkler, M. E.; Rauenbuehler, P.; Wagner, G. *J. Magn. Reson.* **1989**, *82*, 198.
(27) Serianni, A. S.; Podlasek, C. A. *Carbohydr. Res.* **1994**, 259, 277.
(28) (a) Angyal, S. J. *Angew. Chem., Int. Ed. Engl.* **1969**, *8*, 157. (b) Angyal, S. J. *Adv. Carbohydr. Chem. Biochem.* **1984**, *42*, 15. (c) Takagi, S.; Jeffrey, G. A. *Acta Crystallogr.* **1979**, *B35*, 902. (d) Jeffrey, G. A.; McMullan, R. K.; Takagi, S. *Acta Crystallogr.* **1977**, *B33*, 728. (e) Takagi, S.; Jeffrey, G. A. *Acta Crystallogr.* **1977**, *B33*, 3033. (f) Takagi, S.; Jeffrey, G. A. *Acta Crystallogr.* **1978**, *B34*, 1591. (g) Jeffrey, G. A.; Takagi, S. *Acta Crystallogr.* **1977**, *B33*, 738. (h) Takagi, S.; Jeffrey, G. A. *Acta Crystallogr.* **1978**, *B34*, 3104.

(29) Average ^{13}C−^{1}H spin-couplings are presented ±1 std using data found in Tables 2−4.

Table 2. $^{13}C-^{1}H$ Spin-Couplings[a] in Methyl Aldopyranosides Involving C-1

	coupled nuclei					
compound	C1-H1	C1-H2[c]	C1-H3	C1-H5	C1-H5′	C1-CH_3
α-*allo*	169.5	+~1.4	~5.5			4.5
β-*allo*	163.4	−6.5[d]	6.0	~2.1		4.5
β-*altro*	162.4	0	~5.1			4.5
α-*arabino*	161.1 (160.9)[b]	−5.8 (−5.8)		(2.8)		4.5
β-*arabino*	169.7 (169.2)	(br)		~1.9 (2.2)	7.6	4.4
β-*galacto*	160.7	−6.1	1.3	2.5		4.5
α-*gluco*	170.1	+1.0	br	~2.0		4.4
β-*gluco*	161.3	−6.3	1.2	2.3		4.6
α-*manno*	171.0	+~1.2[e]	0	~2.0		4.3
β-*manno*	159.5	+~1.5	0	~2.2		4.5
α-*xylo*	170.1 (169.7)	(0)			(1.7)	
β-*xylo*	161.8 (161.5)	−6.2 (−6.0)	1.1	10.3	2.9 (2.9)	4.5

[a] See footnote (a) in Table 1. [b] Values in parentheses are those observed previously in the corresponding reducing sugar.[40] [c] Indicated sign predicted by the projection rule.[13c] [d] Sign confirmed by the crosspeak displacement method.[26,27] [e] Sign found to be *negative* by the crosspeak displacement method.[26,27] Br denotes broadened signal.

observed coupling (e.g., conversions of α-*allo* to β-*allo* and α-*gluco* to β-*gluco*).

The magnitude of $^{3}J_{C1,H5}$ is expected to depend on the dihedral angle between C-1 and H-5.[13i,j] For compounds containing a C-1−H-5 dihedral angle of ~60° (β-*allo*, β-*galacto*, α-*gluco*, β-*gluco*, α-*manno*, and β-*manno*), $^{3}J_{C1,H5}$ averages 2.2 ± 0.2 Hz (Table 2); in this study only $^{4}C_1$ conformers of D-aldohexopyranosides were examined, thereby limiting observations of $^{3}J_{C1,H5}$ to gauche arrangements. Crystallographic studies yield the following values for $\Theta_{C1,H5}$: β-*galacto* (53.6°),[28c] α-*gluco* (61.5°),[28d] β-*gluco* (55.8°),[28g] and α-*manno* (60.7°).[28d] The variation in $^{3}J_{C1,H5}$ observed in these compounds (Table 2) is consistent with torsional variations observed in the crystal structures, with smaller torsions yielding larger couplings. $^{3}J_{C1,H5(gauche)}$ is on average greater than $^{3}J_{C1,H3(gauche)}$, indicating that the presence of a heteroatom along the coupling pathway enhances coupling, at least for gauche arrangements; it should be noted, however, that $\Theta_{C1,H5(gauche)}$ appears smaller in general than $\Theta_{C1,H3(gauche)}$ (see above), and this factor may also contribute to the observed enhancement. The effect of anomeric configuration on $^{3}J_{C1,H5}$ in aldohexopyranosides is small, that is, coupling appears to be relatively insensitive to the orientation of O-1 with respect to the C-1−O-5−C-5 plane (orienting O-1 in this plane may increase $^{3}J_{C1,H5(gauche)}$ slightly).

Conversion of an aldohexopyranoside to an aldopentopyranoside (i.e., substitution of H for CH_2OH at C-5) enhances $^{3}J_{C1,H5}$. Thus, $^{3}J_{C1,H5(gauche)}$ in β-*gluco* (2.3 Hz) is smaller than the corresponding coupling in β-*xylo* (2.9 Hz); the opposite should be observed if different torsion angles caused this effect, since $\Theta_{C1,H5(gauche)}$ is *smaller* in β-*gluco* (55.8°)[28g] than in β-*xylo* (58.8°).[28e] Interestingly, $^{3}J_{C1,H5(axial)}$ and $^{3}J_{C1,H5(equatorial)}$ in aldopentopyranoses and their methyl glycosides are not highly consistent. Couplings ranging from 1.7−2.9 Hz are observed for gauche arrangements, whereas anti arrangements give values of 7.6 (β-*arabino*) and 10.3 Hz (β-*xylo*) (Table 2). These data suggest that structure at C-1 and C-4 influences $^{3}J_{C1,H5}$ in aldopentopyranosyl rings. Conversions of α- to β-xylopyranoses and β- to α-arabinopyranoses are accompanied by increases in $^{3}J_{C1,H5(gauche)}$ (Table 2). The effect of O-1 orientation on $^{3}J_{C1,H5(gauche)}$ appears more pronounced in aldopentopyranosyl rings than in aldohexopyranosyl rings where it is barely discernable (see above). In crystal structures of methyl xylopyranosides,[28e,h] $\Theta_{C1,H5(gauche)}$ values are 55.2° and 56.7° in the α-anomer (two forms in the unit cell) and 58.8° in the β-anomer, and thus $^{3}J_{C1,H5(gauche)}$ should be *smaller* in the β-anomer if torsion angle were the sole determinant of coupling magnitude. $\Theta_{C1,H5(antiperiplanar)}$ values in β-*arabino* and β-*xylo* are very similar (177.2° and 176.4°, respectively)[28e,f] and thus do not explain the different $^{3}J_{C1,H5(antiperiplanar)}$ observed in these configurations. We conclude that the orientation of O-1 with respect to the C-1−O-5−C-5 plane affects $^{3}J_{C1,H5}$ in aldopentopyranosyl rings, with a coplanar geometry enhancing the coupling.

Table 3. $^{13}C-^{1}H$ Spin-Couplings[a] in Methyl Aldopyranosides Involving C-2

	coupled nuclei			
compound	C2-H2	C2-H1[b]	C2-H3[c]	C2-H4
α-*allo*	142.8	0	−~4.3	0
β-*allo*	143.8	0[f]	−4.6[d]	0
β-*arabino*	146.2	1.1	−5.7	5.3
α-*galacto*	145.9	0.9	−5.7	5.1
β-*galacto*	146.4	0	−~4.8	5.6
α-*gluco*	~145.9			0
β-*gluco*	145.0	0	−4.3	0
α-*manno*	148.5	~1.8[e]	+~1.4[d]	0
β-*manno*	147.9	+7.1	+1.5	0
α-*talo*	149.8	~1.9	+0.8	~4.8

[a] See footnote *a* in Table 1. [b] Couplings are predicted to be zero by the projection rule,[13c] except for β-*manno*. [c] Indicated sign predicted by the projection rule.[13c] [d] Sign confirmed by the crosspeak displacement method.[26,27] [e] Sign found to be negative by the crosspeak displacement method.[26,27] [f] This coupling was found to be +0.3 Hz by the crosspeak displacement method.[26,27]

(b) Couplings Involving C-2. $^{1}J_{C2,H2}$ averages 145.1 ± 1.4 Hz for axial C-2−H-2 bonds and 148.7 ± 1.0 Hz for equatorial C-2−H-2 bonds (Table 3). As observed for $^{1}J_{C1,H1}$, $^{1}J_{C2,H2(axial)} < {}^{1}J_{C2,H2(equatorial)}$, although the difference is smaller than that observed for $^{1}J_{C1,H1}$ and is probably insufficient for reliable use in assigning configuration at C-2 of aldopyranosyl rings.

Coupling between C-2 and H-1 is small (<~1.9 Hz) for rings having the α-*allo*, β-*allo*, β-*arabino*, α-*galacto*, β-*galacto*, β-*gluco*, α-*manno*, and α-*talo* configurations; the projection rule[13c] predicts zero values for these couplings (Table 3). The substitution pattern about the C-1−C-2 bond in all compounds having small $^{2}J_{C2,H1}$, except β-*allo*, β-*galacto*, and β-*gluco*, are identical and thus similar $^{2}J_{C2,H1}$ are expected; $^{2}J_{C2,H1}$ in α-*manno* (~1.8 Hz) was found to have a negative sign by the crosspeak displacement method.[26,27] A different pattern is found in β-*allo*, β-*galacto*, and β-*gluco*, but the *relative* orientation of H-2 with respect to *electronegative* atoms is conserved, and thus small $^{2}J_{C2,H1}$ values are predicted; in β-*allo*, the crosspeak displacement method[26,27] revealed a very small positive $^{2}J_{C2,H1}$ (+0.3 Hz) not observed in 1D spectra. In contrast, the relative orientation of oxygen atoms about the C-1−C-2 bond in β-*manno* results in a large projection sum[13c] (+2.0) and a large positive $^{2}J_{C2,H1}$ (Table 3).

$^2J_{C2,H3}$ values fall within two groups, one showing large absolute couplings (α-*allo*, β-*allo*, β-*arabino*, α-*galacto*, β-*galacto*, and β-*gluco*) (4.9 ± 0.6 Hz) which are predicted to be negative in sign, and the other yielding smaller values (α-*manno*, β-*manno*, and α-*talo*) (1.2 ± 0.4 Hz) which are probably positive in sign (Table 3). Within the former group, α-*allo*, β-*allo*, and β-*arabino* show an identical substitution pattern about the C-2−C-3 bond, whereas α-*galacto*, β-*galacto*, and β-*gluco* show identical substitution of the electronegative atoms (O-2, O-3) with respect to H-3. Using the crosspeak displacement method,[26,27] $^2J_{C2,H3}$ in β-*allo* was found to be negative in sign; it is thus likely that $^2J_{C2,H3}$ is negative in the remaining compounds in this group. Furthermore, configuration at C-4 and possibly C-1 affects the magnitude of $^2J_{C2,H3}$. For example, $^2J_{C2,H3}$ = ~−4.8 Hz in β-*galacto* having O-4 axial and thus antiperiplanar to H-3, whereas a coupling of −4.3 Hz is observed for β-*gluco* (a *trans*-1,2 effect). The conversion of β-*galacto* to α-*galacto* is accompanied by a change in $^2J_{C2,H3}$ from ~−4.8 to −5.7 Hz; the latter coupling is identical to that observed in β-*arabino* which has the same relative configuration at C-1, C-2, C-3, and C-4 as α-*galacto*. These results suggest that 1,3-diaxial interactions (in the present case between O-1 and H-3) affect the magnitudes of $^2J_{CCH}$. Small differences in torsion angles about the C-2−C-3 bond in α-*galacto*, β-*galacto*, and β-*gluco* determined by crystallography[28c,g] do not explain the variations in $^2J_{C2,H3}$; use of these angles and the projection rule[13c] predicts β-*gluco* and β-*galacto* to have the largest and smallest couplings (in absolute value), respectively, contrary to observation. The smaller $^2J_{C2,H3}$ observed in α-*manno*, β-*manno*, and α-*talo* are explained by the different substitution pattern about the C-2−C-3 bond in these compounds and are consistent with predictions.[13c] These couplings are predicted[13c] to have a positive sign; indeed the crosspeak displacement method[26,27] indicates that $^2J_{C2,H3}$ in α-*manno* is positive (Table 3).

Coupling between C-2 and H-4 depends on the C-2−H-4 dihedral angle[13f,l] and is large (5.2 ± 0.3 Hz) in β-*arabino*, α-*galacto*, β-*galacto*, and α-*talo* configurations in which C-2 and H-4 are antiperiplanar or nearly so and very small or zero in α-*allo*, β-*allo*, α-*gluco*, β-*gluco*, α-*manno*, and β-*manno* configurations in which C-2 and H-4 are gauche or nearly so (Table 3). The data suggest that configuration at C-2 does not significantly affect $^3J_{C2,H4}$, at least for the antiperiplanar arrangement (i.e., $^3J_{C2,H4}$ values are similar in α-*galacto* and α-*talo*). Furthermore, the presence of an hydroxymethyl group at C-5 does not affect $^3J_{C2,H4}$ (i.e., couplings are similar in β-*arabino* and α-*galacto* in which $\Theta_{C2,H4}$ are 175.7° and 173.6°, respectively[28c,f]). The different $^3J_{C2,H4}$ in the α- and β-*galacto* configurations cannot be explained by different $\Theta_{C2,H4}$, as crystallographic studies[28c] show a smaller torsion angle (170.9°) in the latter than in the former (173.6°), thereby predicting a larger $^3J_{C2,H4}$ in the α-anomer. The opposite is observed. It should be noted that $^3J_{C1,H3(antiperiplanar)}$ and $^3J_{C2,H4(antiperiplanar)}$ are similar in magnitude (5.5 ± 0.5 and 5.2 ± 0.3 Hz, respectively), indicating that the addition of a second oxygen substituent on the coupled carbon does not appear to significantly affect $^3J_{CCCH(antiperiplanar)}$ values.

(c) **Couplings Involving C-3.** A limited number of $^1J_{C3,H3}$ values were measured, and thus empirical correlations with structure are tentative. Values obtained for axial C-3−H-3 bonds (α-*gluco*, β-*gluco*, and β-*manno*) appear, on average, smaller (143.8 ± 2.4 Hz) than the single value obtained for an equatorial C-3−H-3 bond (β-*allo*) (149.8 Hz) (Table 4), which is consistent with observations made for $^1J_{C1,H1}$ and $^1J_{C2,H2}$. Like $^1J_{C2,H2}$ and unlike $^1J_{C1,H1}$, the magnitude of $^1J_{C3,H3}$ does not change considerably with C−H bond orientation, and thus it is unlikely to be a reliable configurational probe in aldopyranosyl rings.

Table 4. $^{13}C-^1H$ Spin-Couplings[a] in Methyl Aldopyranosides Involving C-3

	coupled nuclei				
compound	C3-H3	C3-H1	C3-H2[b]	C3-H4[b]	C3-H5
β-*allo*	149.8	0	+1.3[c]	+2.1[c]	2.1
α-*gluco*	146.5	5.2	−6.2	−4.3	~2.3
β-*gluco*	142.9	1.1	−4.2	−4.2	2.2
α-*manno*		4.6	−~3.7		
β-*manno*	142.0	0	−4.6	−5.3	2.3

[a] See footnote a in Table 1. [b] Indicated sign predicted by the projection rule.[13c] [c] Sign confirmed by the crosspeak displacement method.[26,27]

Coupling between C-3 and H-1 depends on the C-3−H-1 dihedral angle.[13f,l] Large couplings are observed (4.9 ± 0.4 Hz) in α-*gluco* and α-*manno* configurations where C-3 and H-1 are antiperiplanar (Table 4). $^3J_{C3,H1}$ in α-*gluco* and α-*manno* differ by 0.6 Hz, suggesting that configuration at the intervening C-2 may affect coupling, although the smaller $\Theta_{C3,H1}$ observed in α-*manno* (171.2°)[28d] compared to α-*gluco* (174.5°)[28d] may account for some or all of this difference. Small $^3J_{C3,H1}$ values (<1.1 Hz) are observed in β-*allo*, β-*gluco*, and β-*manno* in which C-3 and H-1 are gauche (Table 4). $^3J_{C3,H1}$ increases when β-*allo* is converted to β-*gluco*, suggesting that the disposition of O-3 with respect to the C-3−C-2−C-1 plane may affect coupling magnitude; since crystallographic data are not available for β-*allo*, it is uncertain whether differences in $\Theta_{C3,H1}$ could account for this effect. Average $^3J_{C3,H1(antiperiplanar)}$ (4.9 ± 0.4 Hz) is similar in magnitude to average $^3J_{C2,H4(antiperiplanar)}$ (5.2 ± 0.3 Hz) and $^3J_{C1,H3(antiperiplanar)}$ (5.5 ± 0.5 Hz), giving an overall average of 5.2 ± 0.4 Hz for $^3J_{CCCH(antiperiplanar)}$. Averaged $^3J_{C3,H1(gauche)}$, $^3J_{C2,H4(gauche)}$, and $^3J_{C1,H3(gauche)}$ data give a value of ~0.7 Hz for $^3J_{CCCH(gauche)}$.

In β-*allo*, $^2J_{C3,H2}$ is small (1.3 Hz) and the projection rule[13c] predicts a positive sign for this coupling which was confirmed experimentally by the crosspeak displacement method[26,27] (Table 4). In contrast, large absolute values (4.7 ± 1.1 Hz) are observed in α-*gluco*, β-*gluco*, α-*manno*, and β-*manno* configurations and these couplings are predicted to have a negative sign. The 2.0 Hz difference between α- and β-*gluco* suggests that configuration at C-1 affects $^2J_{C3,H2}$; the presence of an oxygen (O-1) *anti* to the coupled proton (H-2) enhances $^2J_{C3,H2}$. A similar effect (*trans*-1,2 effect) was observed for $^2J_{C2,H3}$ (see above).

Coupling between C-3 and H-4 in β-*allo* is 2.1 Hz and is predicted to have a positive sign (confirmed experimentally by the crosspeak displacement method[26,27]), whereas $^2J_{C3,H4}$ in α- and β-*gluco* (4.3 Hz) and β-*manno* (5.3 Hz) are predicted to have negative signs. Within the latter group, the larger $^2J_{C3,H4}$ observed in β-*manno* suggests that configuration at C-2 may affect coupling magnitude, possibly due to 1,3-diaxial interactions (between O-2 and H-4) in this configuration. A similar 1,3-diaxial effect was noted for $^2J_{C2,H3}$ (see above).

Coupling between C-3 and H-5 depends on the C-3−H-5 dihedral angle.[13f,l] In this investigation only $^3J_{C3,H5(gauche)}$ was inspected in four compounds (β-*allo*, α-*gluco*, β-*gluco*, and β-*manno*), giving an average value of 2.2 ± 0.1 Hz. These couplings are considerably larger than the closely related $^3J_{C2,H4(gauche)}$ (~0.7 Hz). The different values of $^3J_{C2,H4}$ and $^3J_{C3,H5}$ in *gluco* configurations (Tables 3 and 4) provide evidence that structure at the carbon bearing the coupled proton significantly affects $^3J_{CCCH}$ values; the difference apparently cannot

be attributed to dihedral angle, as $\Theta_{C2,H4} = 65.5°$ and $\Theta_{C3,H5} = 66.3°$ in crystalline α-*gluco*.[28d]

(d) Couplings Involving C-4. With the exception of H-1 and the methyl protons, all of the carbon bound protons of methyl α-D-[4-^{13}C]glucopyranoside are coupled to C-4. In addition to $^1J_{C4,H4}$ (144.0 Hz), $^2J_{C4,H3} = 4.5$ Hz, and $^2J_{C4,H5} = 3.1$ Hz; both two-bond couplings are predicted[13c] to have negative signs. $^3J_{C4,H2} = 0.9$ Hz as expected, since C-4 and H-2 are gauche ($\Theta_{C4,H2} = 62.3°$)[28d] in the α-*gluco* configuration; this coupling appears slightly larger than the related $^3J_{C2,H4}$ ($\Theta_{C2,H4} = 65.5°$)[28d] in the α-*gluco* configuration (Table 3). $^3J_{C4,H6}$ and $^3J_{C4,H6'}$ (H-6′ is defined as the more shielded C-6 proton) are 2.5 and 1.0 Hz, respectively. The latter $^3J_{CH}$ values can be used in conjunction with $^3J_{H5,H6}$ and $^3J_{H5,H6'}$ (Table 1) to assign the H-6 and H-6′ signals stereospecifically (the more shielded C-6 proton is H-6*R*) and to estimate C-5−C-6 rotamer populations (~50/50 *gg*/*gt*).[11c,30]

(e) Couplings Involving C-5. Coupling between C-5 and H-1 is affected by the C-5−H-1 dihedral angle.[13i,j] In previous work,[31] $^3J_{C5,H1}$ was found to be 0.9 Hz in α-D-arabinopyranose and 1.0 Hz in β-D-xylopyranose as expected, since C-5 and H-1 are gauche in these compounds, whereas $^3J_{C5,H1} = 6.1$ and 6.5 Hz in β-D-arabinopyranose and α-D-xylopyranose, respectively, in which C-5 and H-1 are antiperiplanar. In this study, $^3J_{C5,H1}$ values of 6.4 and 0 Hz were observed for α- and β-D-[5-^{13}C]glucopyranoses, respectively, indicating that substitution of CH_2OH for H at C-5 does not significantly alter $^3J_{C5,H1(gauche)}$ or $^3J_{C5,H1(antiperiplanar)}$ values. Gauche and anti couplings across the C-5−O-5−C-1−H-1 coupling pathway (~0.8 and ~6.3 Hz, respectively) are, on average, smaller than corresponding couplings across the C-1−O-5−C-5−H-5 coupling pathway (~2.3 Hz and >7.6 Hz, respectively), indicating that the addition of electronegative groups to the coupled carbon and/or loss of an electronegative substituent on the carbon bearing the coupled proton results in an increase in $^3J_{COCH}$.

In methyl β-D-[5-^{13}C]glucopyranoside, $^3J_{C5,H1} = 0$ Hz ($\Theta_{C5,H1} = 53.8°$),[28g] in agreement with data obtained on the corresponding reducing sugar (see above); in contrast, $^3J_{C1,H5} = 2.3$ Hz (Table 2) despite a slightly larger dihedral angle ($\Theta_{C1,H5} = 55.8°$).[28g] No coupling was observed between C-5 and H-3, which are gauche ($\Theta_{C5,H3} = 69.2°$),[28g] whereas $^3J_{C3,H5}$ is 2.2 Hz (Table 4) with a dihedral angle[28g] of 65.4°. $^2J_{C5,H4} = 4.8$ Hz, and its sign is probably negative. Coupling between C-5 and H-6 (the less shielded C-6 proton) is zero, whereas a 2.4 Hz coupling was observed to H-6′. Finally, $^1J_{C5,H5(axial)} = 142.7$ Hz.

(f) Couplings Involving C-6. In methyl β-D-[6-^{13}C]glucopyranoside, $^1J_{C6,H6} = 144.4$ Hz and $^1J_{C6,H6'} = 143.2$ Hz. Coupling was observed between C-6 and H-5 (~2.1 Hz; sign is affected by C-5−C-6 bond rotation but is predicted to be positive based on the above-noted rotamer populations) and between C-6 and H-4 (3.5 Hz). In the *gluco* configuration, C-6 and H-4 are gauche ($\Theta_{C6,H4} = 51.8°$);[28g] thus $^3J_{C6,H4}$ is substantially larger than $^3J_{CCCH(gauche)}$ values involving *ring* carbons (see above), in part due to a reduced dihedral angle.

(g) Comparison between Related $^2J_{CH}$. A number of $^2J_{CH}$ values have been measured which involve different coupled nuclei yet *apparently* similar coupling pathways. A comparison of these related couplings provides information on the range of values expected for a specific C−C−H coupling pathway geometry within aldopyranosyl rings.

$^2J_{C2,H3}$ in α-*allo* and β-*allo* is governed by the same pathway as $^2J_{C3,H2}$ in α-*manno* and β-*manno* (Figure 2), yet $^2J_{CH}$ values within this group range from ~−3.7 to ~−4.6 Hz. The coupling pathways for $^2J_{C2,H3}$ in α-*manno*, β-*manno*, and α-*talo* are identical to those governing $^2J_{C3,H2}$ and $^2J_{C3,H4}$ in β-*allo* (Figure 3), yet absolute $^2J_{CH}$ values within this group range from 0.8 to 2.1 Hz. Finally, coupling pathways for $^2J_{C2,H3}$ in β-*arabino*, α-*galacto*, β-*galacto* and β-*gluco* are identical to those for $^2J_{C3,H2}$ in α-*gluco*, and β-*gluco*, $^2J_{C3,H4}$ in α-*gluco*, β-*gluco*, and β-*manno*, and $^2J_{C4,H3}$ in α-*gluco* (Figure 4), yet the observed couplings range from −4.2 to −6.2 Hz.

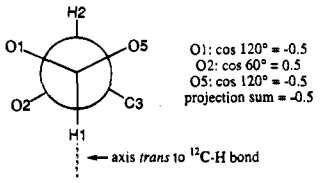

Figure 1. Newman projection about the C-1−C-2 bond of methyl β-D-[1-^{13}C]allopyranoside, showing the reference axis used to compute the projection sum for $^2J_{C1,H2}$.

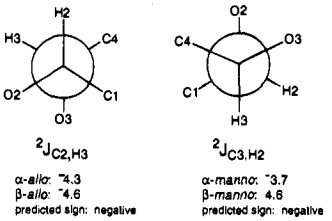

Figure 2. Newman projections about the C-2−C-3 and C-3−C-2 bonds of several aldopyranosyl rings showing similar relative orientation of substituents and similar $^2J_{C2,H3}$ and $^2J_{C3,H2}$, respectively. Experimental couplings and predicted signs[13c] are indicated for each group.

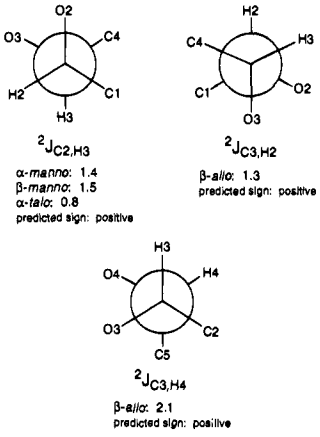

Figure 3. Newman projections about the C-2−C-3, C-3−C-2 and C-3−C-4 bonds in several aldopyranosyl rings showing similar relative orientation of substituents and similar $^2J_{C2,H3}$, $^2J_{C3,H2}$, and $^2J_{C3,H4}$, respectively. Experimental couplings and predicted signs[13c] are indicated for each group.

In these related cases, $^2J_{CH}$ values are similar *but not identical* in magnitude, yielding allowed coupling ranges of 1−2 Hz. This relatively broad range of observed values indicates that *factors in addition to the nature and relative disposition of electronegative substituents on the C−C fragment affect coupling.* These factors probably include differences in bond lengths and angles, ring torsion angles, and/or effects of substituents further removed from the coupling pathway.

(B) ^{1}H Chemical Shifts. (a) Correlations with Ring Structure. Several patterns are observed in the ^{1}H chemical shifts of methyl aldopyranosides (Table 5). As expected, the anomeric (H-1) proton signal appears downfield of those of the remaining carbon-bound protons, although H-1 chemical shifts in ^2H_2O range from 4.354 (α-*arabino*) to 4.969 ppm (α-*talo*). Further inspection of the data in Table 5 suggests a correlation between ^{1}H chemical shift and the disposition of protons on aldopyranosyl rings (i.e., axial vs equatorial). To facilitate

Table 5. ^1H Chemical Shifts[a] of Methyl Aldopyranosides

	nucleus							
compound	H-1	H-2	H-3	H-4	H-5	H-6 (H-5′)	H-6′	OCH_3
α-*allo*	4.875	3.837	4.174	3.701	~3.89	~3.99	~3.85	3.505
β-*allo*	4.691	3.524	4.246	3.699	3.866	3.999	3.789	3.652
β-*altro*	4.879	3.968	4.119	3.987	~3.91	~3.91	3.828	3.627
α-*arabino*	4.354	3.626						3.635
β-*arabino*	4.916	3.926	3.914	4.080	3.958	3.739		3.495
α-*galacto*	4.935	3.917	3.906	4.063	3.997	3.855	3.832	3.511
β-*galacto*	4.413	3.598	3.741	4.019	3.792	3.893	3.848	3.670
α-*gluco*	4.904	3.655	3.761	3.495	3.741	3.965	3.852	3.515
β-*gluco*	4.472	3.358	3.588	3.477	3.560	4.024	3.822	3.670
α-*manno*	4.854	4.024	3.851	3.739	~3.70	3.991	3.852	3.502
β-*manno*	4.658	4.072	3.721	3.652	3.459	4.021	3.825	3.630
α-*talo*	4.969	3.943	3.933	4.009	3.973	3.933	3.869	3.519
α-*xylo*	4.868							
β-*xylo*	4.415	3.345	3.533	3.713	4.064	3.419		3.642

[a] In ^2H_2O, 30 °C; accurate to ±0.002 ppm, except for values reported to only ±0.01 ppm.

Table 6. Average ^1H Chemical Shifts for Equatorial Protons in Methyl Aldopyranosides

ring proton			
H-1	H-2	H-3	H-4
α-*allo*	β-*altro*	α-*allo*	α-*galacto*
β-*arabino*[a]	α-*manno*	β-*allo*	β-*galacto*
α-*galacto*	β-*manno*	β-*altro*	α-*talo*
α-*gluco*	α-*talo*		
α-*manno*			
α-*talo*			
α-*xylo*			
4.903 ± 0.041[b]	4.002 ± 0.058	4.180 ± 0.064	4.030 ± 0.029

[a] H-1 is equatorial in this anomer since the $^1C_4$ ring conformation is preferred by this compound. [b] Average ^1H chemical shifts ±1 std.

discussion of this correlation, chemical shift data have been organized to emphasize these dispositions, and average ^1H chemical shifts have been computed (Tables 6 and 7). Results indicate that the signal of a given ring proton is more shielded when oriented axially than when oriented equatorially. Thus, for example, the average chemical shift of an axial H-1 is 4.555 ± 0.192 ppm[32] (Table 7), whereas that of an equatorial H-1 is 4.903 ± 0.041 ppm (Table 6). Furthermore, a difference in the *errors* associated with the average chemical shifts found in Tables 6 and 7 is observed, with considerably *smaller* standard deviations observed for chemical shifts of equatorial protons. For H-2, H-3, and H-4, this difference may be attributed, in part, to the smaller sampling number for equatorial protons, but other factors, as discussed below, are probably responsible for this behavior. Note the significantly smaller deviation associated with equatorial H-1 chemical shifts (±0.041 ppm) (Table 6) compared to axial H-1 chemical shifts (±0.192) (Table 7) despite an identical sampling number. This observation supports the suggestion that *the chemical shifts of equatorial protons on aldopyranosyl rings are relatively insensitive to ring structure compared to axial protons*, the former being oriented "away" from the ring and therefore less affected by its structure (by inference, it might be expected that equatorial protons will be more affected by intermolecular factors—e.g., solvent effects—than axial protons).

The larger range of ^1H chemical shifts of axial protons may be rationalized by first examining the behavior of H-1. The

(30) Bock, K.; Duus, J. O. *J. Carbohydr. Chem.* **1994**, *13*, 513.
(31) Wu, J.; Bondo, P. B.; Vuorinen, T.; Serianni, A. S. *J. Am. Chem. Soc.* **1992**, *114*, 3499.
(32) Average ^1H chemical shifts are presented ±1 std using data found in Table 5.

Table 7. Average ^1H Chemical Shifts for Axial Protons in Methyl Aldopyranosides

ring proton				
H-1	H-2	H-3	H-4	H-5
β-*allo*	α-*allo*	β-*arabino*	α-*allo*	α-*allo*
β-*altro*	β-*allo*	α-*galacto*	β-*allo*	β-*allo*
α-*arabino*[a]	α-*arabino*	β-*galacto*	β-*altro*	β-*altro*
β-*galacto*	β-*arabino*	α-*gluco*	α-*gluco*	α-*galacto*
β-*gluco*	α-*galacto*	β-*gluco*	β-*gluco*	β-*galacto*
β-*manno*	β-*galacto*	α-*manno*	α-*manno*	α-*gluco*
β-*xylo*	α-*gluco*	β-*manno*	β-*manno*	β-*gluco*
	β-*gluco*	α-*talo*		α-*manno*
	β-*xylo*	β-*xylo*		β-*manno*
				α-*talo*
4.555 ± 0.192[b]	3.643 ± 0.218	3.772 ± 0.144	3.679 ± 0.171	3.789 ± 0.176

[a] H-1 is axial in this anomer since the $^1C_4$ ring conformation is preferred by this compound. [b] Average ^1H chemical shifts ±1 std.

Chart 2. *trans*-1,2 and 1,3-Diaxial Deshielding Effects on the Chemical Shift of an Axial H-1 in an Aldopyranosyl Ring

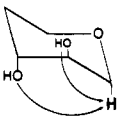

H-1 chemical shifts for α-*arabino*, β-*galacto*, β-*gluco*, and β-*xylo* are very similar and average to 4.414 ± 0.048 ppm (Table 5). The H-1 chemical shifts of β-*allo* (4.691 ppm), β-*altro* (4.879 ppm), and β-*manno* (4.658 ppm) differ considerably from this average, *suggesting that the disposition of hydroxyl substituents with respect to the C-1−H-1 bond may be an important factor in affecting chemical shift.* A deshielding effect of 4.658−4.414 = +0.244 ppm on H-1 results when O-2 is converted from an equatorial to an axial orientation (a *trans*-1,2 effect). A deshielding effect of 4.691−4.414 = +0.277 ppm on H-1 results when O-3 is converted from an equatorial to an axial orientation (a 1,3-diaxial effect). The largest deviation from the average is observed for β-*altro* (+0.465 ppm) as expected, since both *trans*-1,2 and 1,3-diaxial effects contribute to the deshielding of H-1 in this configuration. These deshielding effects are illustrated in Chart 2.

The above-noted structural effects on the chemical shifts of axial anomeric protons are also observed for axial H-2, H-3, H-4, and H-5. The chemical shift average for the equatorial H-2 of β-*altro*, α-*manno*, β-*manno*, and α-*talo* is 4.002 ± 0.058 ppm (Table 6), whereas that for nine compounds having H-2 axial is 3.643 ± 0.218 ppm (Table 7). The larger deviation in the latter average may be attributed to the above-noted *trans*-1,2 and/or 1,3-diaxial effects. For example, the conversion of α-*gluco* to α-*galacto* is accompanied by a +0.262 ppm downfield shift of H-2, and β-*gluco* to β-*galacto* by a +0.240 ppm downfield shift, both attributed to the 1,3-diaxial effect involving O-4. *trans*-1,2 Effects involving O-3 are observed in the conversion of α-*gluco* to α-*allo* (+0.182 ppm) and β-*gluco* to β-*allo* (+0.166 ppm). In a similar vein, conversions of β-*allo* to α-*allo*, β-*galacto* to α-*galacto*, β-*gluco* to α-*gluco*, and α-*arabino* to β-*arabino* are accompanied by +0.30−0.32 ppm downfield shifts of H-2 attributed to the *trans*-1,2 effect involving O-1.

The chemical shift of an axial H-3 is affected by configuration at C-1, C-2, and C-4. Thus, conversions of β-*gluco* to α-*gluco*, β-*galacto* to α-*galacto*, and β-*manno* to α-*manno* are accompanied by downfield shifts of +0.173, +0.165, and +0.130 ppm, respectively, due to the 1,3-diaxial effect of the axial O-1 in α-anomers. The larger downfield shift (+0.381 ppm)

observed in the conversion of β-*xylo* to β-*arabino* is caused by additive 1,3-diaxial and *trans*-1,2 effects.

The average chemical shift of an axial H-4 (3.486 ± 0.013 ppm) is computed from α-*gluco* and β-*gluco* configurations which contain the most shielded H-4 signals due to the absence of *trans*-1,2 and 1,3-diaxial interactions. Conversion to α- or β-*manno*, or α- or β-*allo*, results in +0.17−0.25 ppm downfield shifts of H-4 due to the introduction of 1,3-diaxial (axial O-2) and *trans*-1,2 (axial O-3) effects, respectively. The most deshielded axial H-4 is observed in β-*altro* (+0.501 ppm) where additive *trans*-1,2 (axial O-3) and 1,3-diaxial (axial O-2) effects occur.

Three potential deshielding interactions affect the chemical shift of an axial H-5, namely, those involving O-1, O-3, and O-4. The axial H-5 in β-*gluco* and β-*manno* experiences no deshielding interactions with these oxygens, thus producing the most shielded signals (3.510 ± 0.071 ppm). The chemical shifts of H-5 of α-*allo*, β-*allo*, and β-*altro* average 3.89 ± 0.02 ppm, giving a difference of +0.38 ppm caused by the 1,3-diaxial interaction with O-3. The 1,3-diaxial interaction with O-1 in α-*gluco* and α-*manno* gives an average H-5 chemical shift of 3.72 ± 0.03 ppm (+0.21 ppm), whereas the *trans*-1,2 effect with O-4 in β-*galacto* gives an H-5 chemical shift of 3.792 ppm (+0.28 ppm). The most deshielded H-5 protons are observed in α-*galacto* (3.997 ppm) and α-*talo* (3.973 ppm), giving an average of 3.985 ± 0.017 ppm and a downfield shift of +0.48 ppm. The latter large shift is caused by the additive 1,3-diaxial effect of O-1 (+0.21 ppm) and the *trans*-1,2 effect of O-4 (+0.28 ppm), giving a predicted shift of +0.49, in good agreement with the observed value.

The exocyclic hydroxymethyl protons of methyl aldohexopyranosides are relatively isolated from ring effects and thus their chemical shifts are fairly independent of ring configuration (H-6, 3.958 ± 0.058 ppm; H-6′, 3.837 ± 0.022 ppm) (Table 5). The aglycon methyl proton signals, on the other hand, appear to be affected by anomeric configuration, with axial OCH_3 (3.508 ± 0.009 ppm) being more shielded than equatorial OCH_3 (3.647 ± 0.018 ppm) (Table 5).

(b) Correlations between ^1H and ^{13}C Chemical Shifts. In a previous investigation of ^{13}C chemical shifts in aldoses,[33] the chemical shifts of aldopyranosyl ring *carbons* bearing equatorial hydroxyl groups were found to be considerably more sensitive to ring configuration than those of carbons bearing axial hydroxyl groups. The former are sensitive to configuration at α and β carbons and consistently become *more shielded* as the number of adjacent *axial* hydroxyl groups increases. This observation is consistent with that made for ^1H chemical shifts in this paper in which shifts of axial *protons* (i.e., those attached to carbons bearing equatorial hydroxyl groups) appear more sensitive to ring structure than those of equatorial protons (i.e., carbons bearing axial hydroxyl groups). These results suggest that the sensitivities of the chemical shifts of a given carbon and its directly bonded proton are related, at least in aqueous (^2H_2O) solution.

The above-noted empirical relationships may be extended to provide crude predictions of the ^1H chemical shift behavior in carbohydrates exhibiting greater conformational flexibility than aldopyranosyl rings. For example, conversion of the ^2E form of methyl β-D-ribofuranoside to the ^2E form of methyl β-D-arabinofuranoside should result in a significant downfield shift of the H-1 signal due to the introduction of a *trans*-1,2 effect (with O-2) in the latter (Chart 3). Likewise, conversion of the ^2E form of methyl β-D-xylofuranoside to the ^2E form of methyl β-D-ribofuranoside should induce a downfield shift of the H-1 signal due to the introduction of a 1,3-diaxial effect (with O-3) in the latter (Chart 3).

(33) King-Morris, M. J.; Serianni, A. S. *J. Am. Chem. Soc.* **1987**, *109*, 3501.

Chart 3

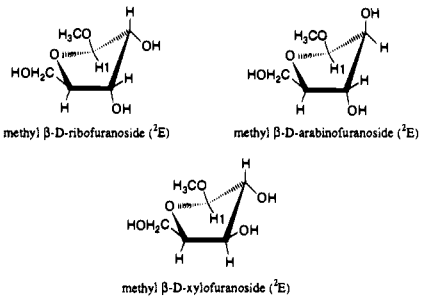

Conclusions

A series of conformationally-rigid aldopyranosyl rings having different configurations was investigated in order to refine empirical relationships between ring structure and configuration, $^{13}C-^1H$ spin-coupling constants, and ^1H chemical shifts. Although several seminal studies of J_{CH} in carbohydrates have been reported,[11-14] couplings involving different carbons within aldopyranosyl rings have not been systematically investigated; one study[15c] has addressed this matter but in acetylated glycosides in nonaqueous solution.

The anticipated importance of $^{13}C-^1H$ spin-coupling constants in future NMR structure determinations of complex carbohydrates enriched either selectively or uniformly with ^{13}C provides an impetus to more thoroughly define their relationships to molecular structure and conformation. Likewise, although numerous ^1H NMR studies of aldopento- and aldohexopyranosyl rings have been reported, the factors controlling ^1H chemical shifts in these monosaccharides are not fully appreciated. This study has revealed several empirical relationships that expand and/or complement the present understanding of J_{CH} and ^1H chemical shifts within aldopyranosyl rings, and these may be summarized as follows.

(a) Results confirm earlier studies[13a,b] showing that $^1J_{C1,H1}$ is sensitive to anomeric configuration, being about 10 Hz larger when H-1 is equatorial than when H-1 is axial. This difference is reasonably consistent, thereby permitting $^1J_{C1,H1}$ to be used reliably to determine the anomeric configuration of aldopyranosyl rings. $^1J_{CH}$ for an equatorial proton at ring carbons other than C-1 is also larger than $^1J_{CH}$ for the same proton in an axial orientation, but the difference is smaller and less consistent than observed for $^1J_{C1,H1}$, making these couplings less reliable for assessing configuration at these sites.

(b) $^2J_{CH}$ values ranging from −6.5 Hz to +7.1 Hz were observed depending on the structure of the C−C−H coupling pathway. The projection rule described by Bock and Pedersen[13c] was obeyed in all compounds investigated in that approximately similar $^2J_{CH}$ (in absolute value) were predicted as were observed experimentally, although sign predictions for small $^2J_{CH}$ are not reliable and thus require experimental verification. In most instances, ranges of couplings were observed for *apparently* identical coupling pathways, indicating that factors other than the nature and relative orientation of electronegative substituents on the C−C fragment affect the observed coupling. These remote effects (*trans*-1,2 and 1,3-diaxial effects) appear most consistent for HO−C−C−H fragments in which the hydroxyl group on the coupled carbon is *equatorial*. In these cases, coupling consistently increases in absolute magnitude when the coupled proton is *trans* to an hydroxyl group located on a carbon β to the coupled carbon and α to the coupled proton. Likewise,

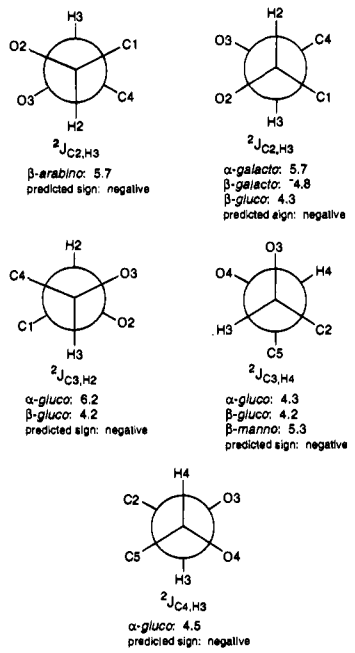

Figure 4. Newman projections about the C-2−C-3, C-3−C-2, C-3−C-4, and C-4−C-3 bonds in several aldopyranosyl rings showing similar relative orientation of substituents and similar $^2J_{C2,H3}$, $^2J_{C3,H2}$, $^2J_{C3,H4}$, and $^2J_{C4,H3}$, respectively. Experimental couplings and predicted signs[13c] are indicated within each group.

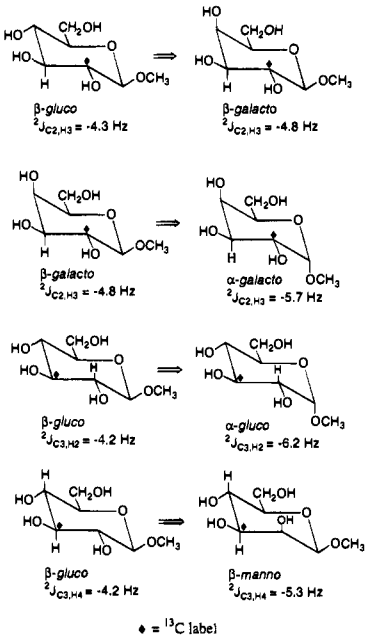

Figure 5. Effect of "remote" hydroxyl group orientation on $^2J_{CH}$ in aldopyranosyl rings. See text for discussion.

in these cases, couplings consistently increase in absolute magnitude when the coupled proton experiences a 1,3-diaxial interaction with an hydroxyl group located on a carbon α to the coupled carbon and β to the coupled proton (Figure 5). The origin of these effects remains obscure.

(c) $^2J_{C1,H2}$ can be used to distinguish between α- and β-anomers having the *arabino*, *allo*, *gluco*, *galacto*, and *xylo* configurations but cannot distinguish between anomers having the *manno* configuration. In the latter case, $^2J_{C2,H1}$ is useful, being small (~−1.8 Hz) in the α-pyranoside and large (+7.1 Hz) in the β-pyranoside. Interestingly, despite different configurations at C-3, $^2J_{C2,H3}$ cannot be used to distinguish between *allo* and *gluco/galacto* configurations. On the other hand, $^2J_{C3,H2}$ is small and positive in *allo* configurations and moderately large

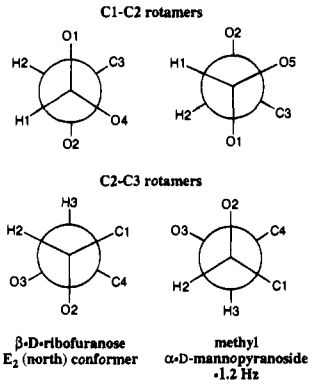

Figure 6. Relationship between the C-1−C-2 and C-2−C-3 Newman projections for the E_2 (north) conformer of β-D-ribofuranose and for methyl α-D-mannopyranoside.

and negative in *gluco* (and presumably *galacto*) configurations. $^2J_{C3,H4}$ can also be used to discriminate between *allo* and *gluco* configurations, being moderately small and positive in the former and moderately large and negative in the latter; although not studied here, $^2J_{C3,H4}$ in *galacto* configurations is expected to be similar in magnitude and sign to $^2J_{C3,H4}$ in *gluco* compounds.

(d) $^3J_{CCCH}$ values are sensitive, as expected, to the torsion angle between the terminal carbon and proton but also to the nature of the intervening atoms and the substituents on these atoms. Average $^3J_{CCCH(gauche)}$ and $^3J_{CCCH(trans)}$ for the C-1−C-2−C-3−H-3 coupling pathway are 0.7 ± 0.7 and 5.5 ± 0.5 Hz, respectively. Corresponding couplings for the C-2−C-3−C-4−H-4, C-3−C-2−C-1−H-1, and C-3−C-4−C-5−H-5 pathways are ~0 Hz and 5.2 ± 0.3 Hz, <1.1 Hz and 4.9 ± 0.4 Hz, and 2.2 ± 0.1 Hz (gauche only), respectively. In *gluco* configurations, $^3J_{C4,H2(gauche)} = 0.9$ Hz, $^3J_{C5,H3(gauche)} = 0$ Hz, and $^3J_{C6,H4(gauche)} = 3.5$ Hz. Variability is thus observed in both gauche and antiperiplanar couplings, but that in the former appears to be larger, which may be due in part to the relative steepness of the Karplus curve for dihedral angles near 60° (compared to that near 180°), although other factors may be involved. The data suggest that the addition of a *second* oxygen substituent on the coupled carbon does not appear to have a large effect on coupling magnitude, at least within the compounds studied (e.g., $^3J_{C1,H3(antiperiplanar)}$ and $^3J_{C2,H4(antiperiplanar)}$ values are comparable). A change in substitution at the carbon bearing the coupled proton, however, can affect $^3J_{CH}$ values significantly. For example, $^3J_{C3,H1(gauche)}$ and $^3J_{C3,H5(gauche)}$ in *β-gluco* are 1.1 and 2.2 Hz, respectively (Table 4), yet $\Theta_{C3,H1} = 56.1°$ and $\Theta_{C3,H5} = 65.4°$ in the crystal.[28g] Based on dihedral angle alone, $^3J_{C3,H1(gauche)}$ should be larger than $^3J_{C3,H5(gauche)}$ if both couplings obeyed the same Karplus relationship. The dihedral angle dependence of $^3J_{C3,H1}$ and $^3J_{C5,H1}$ provides useful information on the anomeric configuration of aldopyranosyl rings complementary to that obtained from $^3J_{HH}$, $^2J_{CH}$, and/or $^1H/^{13}C$ chemical shift.

The presence of an electronegative atom along a vicinal $^{13}C-^1H$ coupling pathway increases coupling for a given dihedral angle relative to $^3J_{CCCH}$. Thus, $^3J_{C1,H5(gauche)}$ averages 2.2 ± 0.2 Hz, whereas $^3J_{C1,H3(gauche)}$ averages 0.7 ± 0.7 Hz, although part of this difference may be attributed to the smaller dihedral angles in the former. Changes in substitution at one or both carbons along a C−O−C−H coupling pathway affect coupling magnitude (e.g., compare $^3J_{C1,H5(gauche)}$ and $^3J_{C5,H1(gauche)}$ in the *β-gluco* configuration). These observations have implications for the interpretation of $^3J_{COCH}$ values across *O*-glycoside linkages of oligosaccharides. The fact that $^3J_{C1,H5}$ may not exhibit the same dependence on dihedral angle as $^3J_{C5,H1}$

indicates a need to exercise caution when interpreting $^3J_{COCH}$ values across linkages having different substitution patterns at one or both carbons along the coupling pathway.

(e) A proton oriented equatorially at a given carbon within an aldopyranosyl ring will, in general, be more deshielded than the same proton oriented axially, regardless of configuration at other ring carbons. This observation is consistent with that made by Lemieux and co-workers[34] in substituted cyclohexanes and sugars, and by Eliel and co-workers[35] in substituted cyclohexanols.

(f) The chemical shifts of equatorial protons in aldopyranosyl rings are much less sensitive to configuration at other ring carbons (i.e., their disposition with respect to hydroxyl substituents on neighboring carbons) than are those of axial protons. It should be appreciated, however, that equatorial protons *are not completely insensitive* to configuration at other ring carbons. For example, in HO−C−C−C−H_{eq} fragments, the disposition of the OH group affects the chemical shift of the equatorial H_{eq}; in such arrangements, the H_{eq} signal is consistently more shielded (~−0.06 ppm) when the OH group is axial (e.g., H-3 is more shielded in α-*allo* than in β-*allo*; Table 5). A similar effect has been observed in substituted cyclohexanes.[34]

(g) Two structural motifs appear to uniformly affect axial proton chemical shifts regardless of position in an aldopyranosyl ring, and both cause deshielding. An hydroxyl group *trans* to an axial ring proton deshields the latter (a *trans*-1,2 effect), whereas an hydroxyl group in a 1,3-diaxial position with respect to a ring proton deshields the latter (a 1,3-diaxial effect). The magnitude of deshielding induced by these effects ranges from ~0.2−0.4 ppm. Similar effects have been reported in cyclohexane derivatives by Danneels and Anteunis.[36,37]

The results of this study should provide a firmer basis on which to interpret $^1J_{CH}$, $^2J_{CH}$, and $^3J_{CH}$ values in ^{13}C-labeled biologically-important oligosaccharides in structural terms. In addition, however, ^{13}C−^{1}H couplings in aldopyranosyl rings may be used to provide approximate couplings *in specific forms* of more conformationally flexible aldopyranosyl rings (e.g., α-*ido*) and aldofuranosyl rings where structural analysis is complicated by the presence of conformational averaging in solution. For example, $^2J_{C1,H2}$ in north (E_2) conformations of the β-D-ribofuranose ring can be *approximated* by $^2J_{C1,H2}$ in methyl α-D-mannopyranoside, since the relative orientations of substituents at C-1, C-2, and C-3 in these structures are similar (axial−axial−equatorial; Figure 6).[38] Likewise, $^2J_{C1,H2}$ in methyl β-D-allopyranoside approximates $^2J_{C1,H2}$ in south (^2E) conformations. These correlations, while imperfect,[39] should nevertheless provide a means to establish realistic limits on specific J_{CH} values in discrete conformers of aldofuranose rings. This latter information may facilitate the structural interpretation of J_{CH} values in ^{13}C-labeled RNA, DNA, and oligosaccharides that contain furanose constituents.

Acknowledgment. This work was supported by a grant from Omicron Biochemicals Inc., South Bend, IN.

JA950309W

(34) Lemieux, R. U.; Kullnig, R. K.; Bernstein, H. J.; Schneider, W. G. *J. Am. Chem. Soc.* **1958**, *80*, 6098.

(35) Eliel, E. L.; Gianni, M. H.; Williams, Th. H. *Tetrahedron Lett.* **1962**, *17*, 741.

(36) Danneels, D.; Anteunis, M. *Tetrahedron Lett.* **1975**, *9*, 687.

(37) Anteunis, M.; Danneels, D. *Org. Magn. Reson.* **1975**, *7*, 345.

(38) Serianni, A. S. in *NMR of Biological Macromolecules,* Stassinopoulou, C. I., Ed.; NATO ASI Series H: Cell Biology, Springer-Verlag: 1994; Vol. 87, pp 293−306.

(39) Furanose rings are not puckered to the same extent as pyranosyl rings, and thus ideal staggered C−C rotamers such as those employed in this paper are not strictly applicable. This imperfect staggering of substituents will affect the magnitudes of J_{CH}. In addition, ring strain differences between furanosyl and pyranosyl rings, which translate into different bond lengths and angles, will also affect J_{CH} values.

(40) Wu, G. D.; Serianni, A. S.; Barker, R. *J. Org. Chem.* **1983**, *48*, 1750.